Charge-state-correlated cross sections for electron loss, capture, and ionization in C^{3+}-Ne collisions

T. Kirchner,[1,*] A. C. F. Santos,[2] H. Luna,[3] M. M. Sant'Anna,[2] W. S. Melo,[4] G. M. Sigaud,[3] and E. C. Montenegro[3]
[1]*Institut für Theoretische Physik, TU Clausthal, Leibnizstraße 10, D-38678 Clausthal-Zellerfeld, Germany*
[2]*Instituto de Física, Universidade Federal do Rio de Janeiro, Cx. Postal 68528, Rio de Janeiro 21941-972, Brazil*
[3]*Departamento de Física, Pontifícia Universidade Católica do Rio de Janeiro, RJ 22452-970, Brazil*
[4]*Departamento de Física, Universidade Federal de Juiz de Fora, Juiz de Fora 36036-330, Brazil*
(Received 2 March 2005; published 12 July 2005)

Charge-state-correlated total cross sections for projectile-electron loss, capture, and target ionization in C^{3+}-Ne collisions have been measured and calculated at absolute energies in the few MeV regime. The calculations are based on a recently proposed coupled mean-field approach which combines a set of nonperturbative single-particle calculations for the initial projectile electrons with another one for the initial target electrons. The basis generator method has been used to solve these equations. Very good overall agreement between experimental and theoretical data is found, which provides further evidence for the applicability of the approach to rather complex many-electron collision systems. One notable exception is the cross section for elastic projectile-electron loss associated with no change of the target charge state. In this case, the theoretical and experimental results differ qualitatively.

DOI: 10.1103/PhysRevA.72.012707 PACS number(s): 34.10.+x, 34.50.Fa, 34.70.+e

I. INTRODUCTION

Charge-changing processes in ion-atom collisions with active electrons on both nuclei have been studied extensively for many years. They are of interest in different research fields, e.g., plasma physics [1] and accelerator technology [2], and, in particular, for current projects related to nuclear fusion and nuclear reactions involving radioactive beams, where electron removal processes from dressed projectile ions cause undesired beam transport losses and losses in storage rings (see, e.g., Refs. [3–5] and references therein). From the more fundamental atomic physics perspective these collision systems have attracted considerable attention, since a multitude of different processes, such as single and multiple excitation, ionization, and electron transfer between both centers can occur and compete with each other, i.e., interesting many-electron dynamics can be expected.

A natural starting point for the theoretical analysis of these processes is, of course, perturbation theory. It was first applied by Bates and Griffing to collisions between two hydrogen atoms half a century ago [6–8], and has been elaborated and extended to other systems by several authors (see, e.g., Refs. [9,10]). In particular, two first-order processes leading to projectile-electron loss can be distinguished in this framework, since they are associated with different transition amplitudes, (i) an interaction of a projectile electron with the (screened) target nucleus (so-called screening mode); (ii) an interaction of a projectile electron with one of the target electrons, which is also excited or ionized (so-called antiscreening mode) [9,10]. It was possible to verify this separation experimentally for fast projectile-ion impact on atomic and molecular targets [11–13], most clearly by measuring the momentum distributions of the recoil ions, which are very different for the screening and antiscreening modes [14–16]. The latter process has recently been suggested as a means of studying the mechanisms of electron-impact ionization $(e,2e)$ of ions [17], for which real electron-ion collision experiments are difficult.

Perturbative methods gradually lose their validity for heavier systems and towards lower collision energies, where the interactions are in general stronger and the competition and coupling of different reaction channels become important. In this regime, classical trajectory Monte Carlo methods have been applied with some success, in particular for the heavy-ion collision systems of interest for the above-mentioned nuclear physics projects [18], but also for lighter projectile ion impact (see, e.g., Refs. [19,20]). The latter situation was also considered in the framework of the so-called free-collision model (also referred to as classical impulse approximation) [21,22], in which projectile electron loss is described as an elastic electron scattering event. More rigorous nonperturbative quantum calculations are relatively rare and have been mostly restricted to situations in which electron transfer can be neglected [23–25].

Experimentally, regions in which electron transfer competes with ionization and projectile-electron loss have been clearly identified, e.g., in Ref. [26] for He^+, and in Ref. [22] for C^{3+} and O^{5+} projectiles. However, such situations have not been addressed in terms of quantum-theoretical approaches until very recently. In the last few years, He^+ collisions with neon and argon atoms have been investigated in closer detail and over broader ranges of impact energies from a few keV/amu to 1 MeV/amu [27–30]. These works are based on two different sets of nonperturbative mean-field calculations; one for the initial projectile electron, and one for the initial target electrons. Charge-changing cross sections have been computed by statistical combinations of the resulting single-particle transition amplitudes. While the procedure was motivated by a rather intuitive physical picture

*Electronic address: tom.kirchner@tu-clausthal.de

(and an obvious approximation of the full time-dependent Hartree-Fock equations) [27], the use of different mean fields for both types of electrons has a notable drawback; the time-developed projectile and target orbitals lose their initial orthogonality. This cannot be remedied easily, but it can be taken into account in terms of a renormalization procedure in the analysis of the single-particle solutions [28–30]. It was found that this is particularly important at low impact energies, where electron transfer into $He(1s^2)$ is strong. Furthermore, it turned out that a reliable calculation of this capture process requires consideration of the Pauli exclusion principle to account for the spin-singlet structure of the final two-electron state [28,30].

These works have been rather successful. To our knowledge they represent the most sophisticated quantum-mechanical calculations that have been applied to this kind of problem so far. In order to test the validity of the approach further and to shed light on the above-mentioned competition between different reaction channels we address the C^{3+}-Ne collision system at absolute energies in the few MeV regime in the present work. We present the first theoretical and experimental total cross sections for single-electron transfer, pure ionization, and single projectile-electron loss determined in coincidence with the final charge states of the recoil ions. The theoretical approach is summarized in Sec. II, while the main features of the experimental apparatus as well as the experimental results are presented in Sec. III. Calculations and measurements are compared in Sec. IV, and some conclusions are drawn in Sec. V. Atomic units ($\hbar = m_e = e = 1$) are used unless otherwise specified.

II. THEORY

Our theoretical description of the ion-atom collision system is based on the semiclassical approximation, in which the heavy-particle motion is characterized by a classical (straight line) trajectory $\mathbf{R}(t)$. As mentioned in the Introduction, a coupled mean-field description of initial projectile and target electrons is used, since the explicit solution of the many-electron time-dependent Schrödinger equation (TDSE) is illusory in the nonperturbative realm. The treatment can be regarded as an approximate time-dependent Hartree-Fock (TDHF) [31] or density functional theory (TDDFT) [32,33] description, whose more refined versions have so far only been applied to collision systems which involve electrons bound initially to one center [34–37].

A. Mean-field models for projectile and target electrons

The starting point of our treatment is the definition of two different single-particle Hamiltonians for the time development of the initial target and projectile electrons. For the N_T initial target electrons we consider

$$i\partial_t \psi_i(\mathbf{r},t) = \hat{h}_T(t)\psi_i(\mathbf{r},t), \quad i = 1,\ldots,N_T, \tag{1}$$

with the Hamiltonian

$$\hat{h}_T(t) = -\frac{1}{2}\Delta + \left(-\frac{Q_T}{r_T} + v_{ee}^T(r_T,t)\right) + \left(-\frac{Q_P}{r_P} + v_H^P(r_P)\right). \tag{2}$$

Q_T and Q_P are the charges of the target and projectile nuclei, and r_T and r_P denote the distances of the active electron to the target and projectile centers, respectively. The target center is chosen as the origin of the reference frame such that $r_P = r_P(t) = |\boldsymbol{r}_T - \boldsymbol{R}(t)|$. The effective potentials in Eq. (2) account for the interaction of a target electron with the other target electrons (v_{ee}^T) and with the projectile electrons (v_H^P), and are specified further below.

For the N_P projectile electrons we consider

$$i\partial_t \psi_i(\mathbf{r},t) = \hat{h}_P(t)\psi_i(\mathbf{r},t), \quad i = N_T+1,\ldots,N = N_T+N_P, \tag{3}$$

with the Hamiltonian

$$\hat{h}_P(t) = -\frac{1}{2}\Delta + \left(-\frac{Q_P}{r_P} + v_{ee}^P(r_P)\right) + \left(-\frac{Q_T}{r_T} + v_H^T(r_T)\right) \tag{4}$$

in the projectile reference frame with $r_T = r_T(t) = |\boldsymbol{r}_P - \boldsymbol{R}(t)|$.

The effective potentials in both Hamiltonians (2) and (4) are chosen so that the situation before the collision is described accurately, while time-dependent variations are taken into account only in v_{ee}^T via the ansatz

$$v_{ee}^T(r_T,t) = v_{ee}^T(r_T) + \delta v_{ee}(r_T,t), \tag{5}$$

$$\delta v_{ee}(r_T,t) = \frac{-1}{N-1}\sum_{q=1}^{N}(q-1)P_q^{\mathrm{loss}}(t)v_{ee}^T(r_T), \tag{6}$$

which was suggested in Ref. [38] as a global model for the increasing attraction of the target as q electrons are removed during the collision with probabilities P_q^{loss}.

The stationary potentials have been obtained from the so-called exchange-only version of the optimized potential method (OPM) of ground-state DFT [39,40]. This means that accurate Hartree (H) and exchange (x) contributions are included in v_{ee}^T and v_{ee}^P, while pure Hartree potentials are used for v_H^T and v_H^P,

$$v_{ee}^{T(P)}(r_{T(P)}) = v_H^{T(P)}(r_{T(P)}) + v_x^{T(P)}(r_{T(P)}). \tag{7}$$

The different choices in Eqs. (2) and (4) are dictated by the fact that exchange between projectile and target electrons does not contribute at large internuclear separations, and by the asymptotic properties,

$$v_{ee}^{T(P)}(r_{T,(P)}) \overset{r_{T(P)}\sim\infty}{\sim} \frac{N_{T(P)}-1}{r_{T(P)}}, \tag{8}$$

$$v_H^{T(P)}(r_{T,(P)}) \overset{r_{T(P)}\sim\infty}{\sim} \frac{N_{T(P)}}{r_{T(P)}}, \tag{9}$$

which ensure that all electrons experience the correct asymptotic charges on both centers before the collision. The price one has to pay for choosing $\hat{h}_T(t) \neq \hat{h}_P(t)$ is that the propagated target and projectile orbitals lose their orthogo-

nality in the course of the collision. This deficiency cannot be avoided, unless accurate time-dependent two-center OPM or nonlocal TDHF potentials would be constructed and used. This is, however, much more demanding than the present model. The practical advantage of our scheme is that Eqs. (1) and (3) are dynamically uncoupled and can be solved independently. The nonorthogonality is not ignored, but considered in the final-state analysis (see Sec. II C).

Of course, the procedure cannot be regarded as a first-principles scheme, but its practical successes have corroborated its usefulness for applications. From a physical point of view our model includes screening-mode-type processes to all orders, since the interaction of a projectile or target electron with the screened potential on the other center is fully taken into account. By contrast, ionization by explicit electron-electron interaction (antiscreening) cannot be described in the framework of single-particle equations, unless time-dependent correlation effects would be included in the potentials. While this is in principle possible from the viewpoint of TDDFT, practicable schemes virtually do not exist.

B. Solution of the single-particle equations

The single-particle equations (1) and (3) have been solved by using the nonperturbative basis generator method (BGM) [41,42]. As in the previous works for He^+ impact on atoms [27–30], separate calculations have been performed for the initial projectile and target electrons for each set of collision parameters.

The BGM is a coupled-channel method, in which the basis is constructed by repeated application of (regularized) Coulomb potentials onto atomic eigenfunctions,

$$\psi_i^{T(P)}(\mathbf{r},t) = \sum_{\mu=0}^{M_{T(P)}} \sum_{v=1}^{V_{T(P)}} c_{\mu v}^{i,T(P)}(t)\chi_v^{\mu,T(P)}(\mathbf{r},t), \tag{10}$$

$$\chi_v^{\mu,T(P)}(\mathbf{r},t) = [W_{P(T)}(r_{P(T)})]^{\mu}\varphi_v^{T(P)}(\mathbf{r}), \quad \mu = 0,\ldots,M_{T(P)}, \tag{11}$$

$$W_{P(T)}(r_{P(T)}) = \frac{1}{r_{P(T)}}[1-\exp(-r_{P(T)})], \tag{12}$$

where $\psi_i \equiv \psi_i^T$ if $i \in \{1,\ldots,N_T\}$ and $\psi_i \equiv \psi_i^P$ if $i \in \{N_T+1,\ldots,N=N_T+N_P\}$ [cf. Eqs. (1) and (3)]. The scheme is motivated by the insight that the model spaces built in this way are dynamically adapted to the time development of the systems [42], and reasonable convergence can be achieved with comparably small basis sets. For the active target orbitals we have used the same expansion as in our previous works, which consists of all atomic eigenfunctions of the *KLMN* shells and 100 functions from the set $\{\chi_v^{\mu,T}(\mathbf{r},t), \mu = 1,\ldots,M_T=8\}$. For the active projectile orbitals we have used a similar basis that includes all eigenfunctions of the ground state C^{3+} ion from the *KLMN* shells and 79 functions from the set $\{\chi_v^{\mu,P}(\mathbf{r},t), \mu=1,\ldots,M_P=8\}$. The choices were guided by calculating the correlation diagram of the (frozen) quasimolecular system $(CNe)^{3+}$ within the basis sets.

All orbitals have been propagated from an initial separation between projectile and target nuclei of 15 a.u. to the same final distance, and 23 impact parameters between $b_{\min}=0.2$ a.u. and $b_{\max}=12$ a.u. have been considered for each impact energy. This proved to be sufficient to guarantee a numerical accuracy of the results of about 1%–2%.

C. Analysis of electron removal processes

In this work we wish to calculate probabilities and cross sections for single- and multiple-electron transitions. A well-established method to extract these quantities from the solutions of single-particle equations is the *inclusive probabilities* formalism of Lüdde and Dreizler [43], which starts from the assumption that both final and time-propagated states are represented by single Slater determinants. Because of the nonorthogonality of the propagated projectile and target orbitals some care must be taken to ensure normalization of the many-electron states. With the overlap integrals

$$S_{ji}(t) = \langle \psi_j(t) | \psi_i(t) \rangle \tag{13}$$

a normalized N-electron wave function is given by

$$\Psi(x_1,\ldots,x_N;t) = \frac{\det[\phi_1(x_1,t),\ldots,\phi_N(x_N,t)]}{\sqrt{N!\det[S_{11}(t),\ldots,S_{NN}(t)]}}, \tag{14}$$

where the ϕ_i denote spin orbitals

$$\phi_i(x,t) = \psi_i(\mathbf{r},t)\chi_{\sigma_i}(s) \tag{15}$$

with spatial parts $\psi_i(\mathbf{r},t)$ and standard spin functions $\chi_{\sigma_i}(s)$ [28]. Note that in the present case of $N=N_T+N_P$ target and projectile electrons, nonvanishing overlaps occur only for pairs of propagated target and projectile orbitals, while target and projectile orbitals are orthogonal among each other

$$S_{ji}(t) = \delta_{ji} \quad \text{if } j,i \in \{1,\ldots,N_T\} \quad \text{or } j,i \in \{N_T+1,\ldots,N\}. \tag{16}$$

Using Cramer's rule one can show that the corresponding renormalized one-particle density matrix is given by

$$\hat{\gamma}^1(t) = \sum_{i,j=1}^{N} |\psi_i(t)\rangle S_{ij}^{-1}(t)\langle\psi_j(t)|, \tag{17}$$

where S_{ij}^{-1} denotes the (i,j)th element of the inverse overlap matrix. The inclusive probability $P_{f_1,\ldots,f_q}$ of finding $q<N$ electrons in specific states, labeled by $f_1,\ldots,f_q$, while nothing is known about the final states of the other electrons, can then be expressed as a $q\times q$ determinant of $\hat{\gamma}^1$ in the standard way [43],

$$P_{f_1,\ldots,f_q} = \det(\langle f_1|\hat{\gamma}^1|f_1\rangle \cdots \langle f_q|\hat{\gamma}^1|f_q\rangle). \tag{18}$$

With the definition

$$\tilde{P}_{mn} = \sum_{f_1<,\ldots,<f_m}^{P} \sum_{f_{m+1}<,\ldots,<f_{m+n}}^{T} P_{f_1,\ldots,f_{m+n}}, \tag{19}$$

in which the first and second summations are over all bound projectile and target states, respectively, the probability to find *exactly* k electrons on the projectile and l electrons on the target is given by [44] (see also Ref. [45])

$$P_{kl} = \sum_{mn} (-1)^{m-k+n-l} \binom{m}{m-k} \binom{n}{n-l} \tilde{P}_{mn},$$

$$m \geqslant k, \quad n \geqslant l, \quad m+n \leqslant N. \tag{20}$$

These ordered sums of the basic inclusive probabilities (18) have been evaluated at the final time $t=t_f$ in order to calculate probabilities and cross sections for charge-state-correlated events. As the number of determinants increases rapidly with an increasing number of states we have restricted the summations to the *KLMN* shells of the projectile and the *KLM* shells of the target to represent the bound contributions. However, we have checked that the *N* shell of the target is populated only weakly so that its omission in the analysis does not introduce significant errors.

III. EXPERIMENT

The experimental apparatus has been described in detail previously [22,46–50] and only the main features are outlined here. In brief, C^+ ion beams ranging from 1.0 to 3.5 MeV were delivered by the 4 MV Van de Graaff accelerator of the Pontifícia Universidade Católica do Rio de Janeiro and passed through a gaseous stripper, producing a C^{3+} beam. The C^{3+} beam was momentum analyzed by a switching magnet being directed into a gas cell. Apertures of 1.5 mm and 2.0 mm in diameter define the entrance and exit of the cell. The cylinder-shaped gas cell with 1.4 l volume is large enough to ensure that the pressure measurements inside the cell, made by an absolute capacitive manometer, are not affected by the leak through the apertures towards the differentially pumped region. The emergent beams, C^{2+}, C^{3+}, and C^{4+} were charge analyzed by a second magnet and recorded either by two surface barrier detectors (SB) or by a position-sensitive microchannel plate detector (MCP-*xy*) housed in a detection chamber placed 4 m downstream from the target region. The counting rates were kept below 1.5×10^3 and 3×10^2 counts/s, for the SB and MCP-*xy* detectors, respectively, to prevent pile-up (in the surface barriers) or local saturation (in the microchannel plate) effects. The higher counting rates supported by the SB detector made the calibration of the recoil-ion efficiency more accurate. On the other hand, especially for the lower projectile energies, the MCP-*xy* images were important to identify and exclude contributions from spurious beams formed before the gas cell by charge-changing collisions with the background gases. In principle, double- and triple-electron capture and loss—corresponding to C^+, C^{2+}, C^{5+}, and C^{6+} emergent beams, respectively—could also be simultaneously measured using this arrangement. However, their cross sections are too low to make these measurements feasible with this setup.

The measurements using the SB detectors were made in two steps. First, both the capture and direct ionization channels were recorded simultaneously. In the second step the direction of the charge-analyzing magnet was reversed, and both the loss and direct ionization channels were measured. In both steps, the main beam (direct ionization) was recorded by the same SB detector.

One could observe that, for the emergent particle beams other than the main beam, a horizontal broadening in their shapes occurs. This broadening is due to the deflection by the pushing static electric field in the interaction region. As the broadening increased for lower projectile velocities, the measurements using the SB detectors at lower energies differed from those using the MCP-*xy*, due to the different fractions lost by the emergent beams in the SB detectors. This point is worth mentioning because this broadening can be quite significant when a combination of low-energy and highly-charged projectile is used in this kind of measurement. As this effect increases with the charge state, the loss channel is more affected compared with the ionization or capture ones. The reported cross sections are, for that reason, based on the MCP-*xy* measurements. On the other hand, for energies above 2.5 MeV, both sets of measurements agree with each other. This effect would also make the measurements of the charge states higher than C^{4+} more difficult, due to the overlap of the emergent beams.

The multiply ionized recoil ions produced by the primary beam, under single collision conditions, were accelerated by a two-stage extraction electric field and detected by a microchannel-plate detector in a chevron configuration. This recoil-ion detector provided the stop signals to two time-to-amplitude converters started by the signals from either the SB or the MCP-*xy* detectors, in a standard time-of-flight setup.

Special care was taken to obtain the detection efficiencies of the multiply charged recoil ions. This was achieved by measuring the recoil ions in coincidence with the C^{2+} projectiles (single capture collision channel) as well as the projectile yields for the total single-electron capture collision channel [46,47]. The set of recoil efficiencies were found to be virtually independent of the charge states and masses of the recoil ions. The total single-electron capture cross sections σ_{32} of C^{3+} on Ne can be, thus, obtained through the measurements of several charge states,

$$\sigma_{32} = \sum_q \sigma_{32}^{q+}, \tag{21}$$

which were compared to the data of Ref. [22], which are single measurements, with no recoil ions being measured. The good agreement, within the experimental uncertainties, between these two measurements, carried out through different methods, corroborates the independence of the efficiency from the recoil-ion detection.

The main sources of uncertainties in the coincidence measurements come from impurities in the gas targets due to the

TABLE I. Absolute multiple-ionization cross sections of Ne by C^{3+} ions, pure ionization channel (Mb).

E (MeV)	Ne^+	Ne^{2+}	Ne^{3+}	Ne^{4+}
1.0	231±23	56±8	22±4	7.4±2.6
1.5	281±22	68±7	34±4	9.0±1.4
2.0	313±22	73±8	34±5	12±2
2.5	295±24	74±7	28±4	12±3
3.0	372±56	93±15	40±8	13±3
3.5	359±54	87±14	35±7	12±3

TABLE II. Absolute multiple-ionization cross sections of Ne by C^{3+} ions, transfer-ionization channel (Mb).

E (MeV)	Ne^{+}	Ne^{2+}	Ne^{3+}	Ne^{4+}
1.0	272±24	136±16	49±7	13±3
1.5	135±17	95±14	48±9	14±4
2.0	87±9	75±9	36±5	14±3
2.5	63±7	52±6	23±3	13±3
3.0	66±10	45±5	21±4	10±3

gas-admittance system (~1%–3%), the determination of the product of the detection efficiency by the effective length of the gas cell (~10%), fluctuations in the gas cell pressure (~5%), counting statistics, and random coincidence subtraction (up to ~15%). The overall uncertainties range between 15% and 35%. Tables I–III present our results.

IV. RESULTS AND DISCUSSION

The experimental and theoretical charge-state-correlated total cross sections for pure ionization, transfer ionization, and loss-ionization are compared in Figs. 1–3. We note that post-collisional Auger-type processes have not been taken into account in the calculation, since they are expected to be minor in the range of impact energies considered. This can be inferred from previous investigations of such processes, which showed that they are most important at higher projectile velocities [50–52], and from the fact that the removal of a Ne K-shell electron, which would give rise to a strong Auger process, is rather unlikely in the present kinematical regime according to our calculation.

Figure 1 shows the cross sections for pure multiple ionization of Ne. Very good agreement between measured and calculated values is observed for all recoil-ion charge states $q=1,\ldots,4$. The cross sections increase slowly as a function of the projectile kinetic energy E_P. According to the calculations (which were extended to energies higher than those displayed in Fig. 1), the cross sections reach their maximum values at $E_P \approx 5$ MeV.

Figure 2 shows the cross sections for q-fold target ionization associated with single capture. The overall agreement is also good, but some deviations between experimental and theoretical results are noticeable. Below $E_P=2$ MeV and for $q \geqslant 2$, the calculations have the tendency to lie below the

TABLE III. Absolute multiple-ionization cross sections of Ne by C^{3+} ions, loss-ionization channel (Mb).

E (MeV)	Ne^{+}	Ne^{2+}	Ne^{3+}	Ne^{4+}
1.0	8.6±0.9	5.4±0.6	1.6±0.3	0.9±0.2
1.5	11±1	7.3±0.9	3.0±0.5	1.5±0.3
2.0	13±1	10±1	5.0±0.6	2.3±0.4
2.5	13±2	11±1	4.9±0.6	2.7±0.4
3.0	16±3	11±2	6.3±1.1	2.5±0.6
3.5	14±2	10±2	5.7±1.0	2.5±0.6

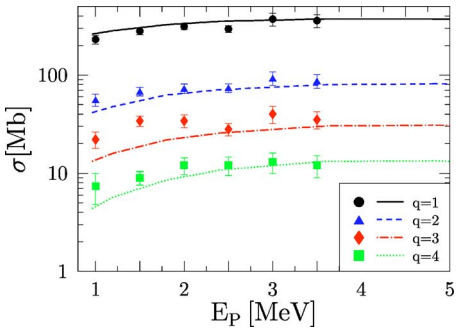

FIG. 1. (Color online) Absolute multiple-ionization cross sections of Ne by C^{3+} ions as functions of the projectile kinetic energy, pure ionization channel. The lines represent the theoretical results, and the symbols represent measured values for recoil ion charge states $q=1,\ldots,4$.

measured values. A similar trend was observed earlier for transfer ionization in He^{2+}-Ne collisions [38], and was attributed to limitations of the multinomial analysis of the propagated orbitals used in that study. This was inferred from the fact that pure single capture and pure single ionization were in good agreement with experiments so that their product should also agree with measurements, if transfer ionization would really be dominated by independent interactions. Although the present analysis in terms of inclusive probabilities is more sophisticated, it is also based on the assumption of independent electrons, i.e., on single determinantal wave functions. We have checked that the multinomial models used in Ref. [38] yield similar results. We did not include them in the figures as their applicability is questionable on theoretical grounds in the case of nonorthogonal orbitals. Whether the independent electron analysis is problematic in the present case could be better judged if the comparison could be extended towards lower impact energies, where the discrepancies observed in Ref. [38] were much more pronounced. However, those measurements were not feasible in the current setup.

The other discrepancy concerns the pure capture channel ($q=1$) at intermediate impact energies, where the theoretical results lie above the experimental ones. Given that single-electron transitions are typically best described by mean-field

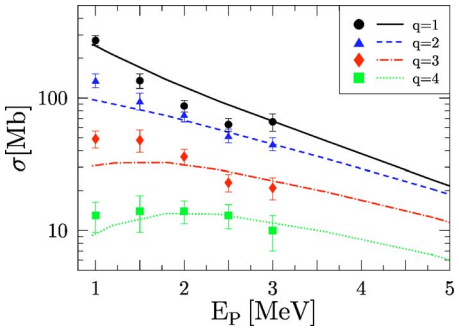

FIG. 2. (Color online) Absolute multiple-ionization cross sections of Ne by C^{3+} ions as functions of the projectile kinetic energy, transfer-ionization channel. The lines represent the theoretical results, and the symbols represent measured values for recoil ion charge states $q=1,\ldots,4$.

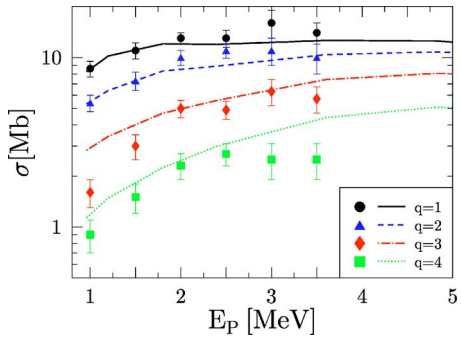

FIG. 3. (Color online) Absolute multiple-ionization cross sections of Ne by C^{3+} ions as functions of the projectile kinetic energy, loss-ionization channel. The lines represent the theoretical results, and the symbols represent measured values for recoil ion charge states $q=1,\ldots,4$.

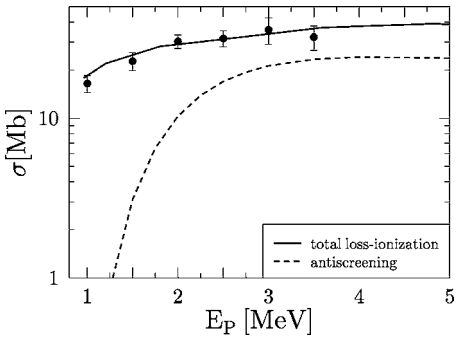

FIG. 4. Absolute cross section for total loss-ionization σ_{34}^{i} (22) in C^{3+}-Ne collisions as a function of the projectile kinetic energy. The full line represents the results of the coupled mean-field calculation, the dashed line the results of the PWBA calculation for the antiscreening mode, and the symbols represent measured values for σ_{34}^{i}.

models, this discrepancy is difficult to understand.

In Fig. 3 we compare our results for the loss-ionization channel. The overall agreement is very convincing in this case as well. This is remarkable, because loss-ionization can be caused by the antiscreening mechanism mentioned in the Introduction, which is not taken into account in our theoretical model. Apparently, the data of Fig. 3 give no indication that antiscreening contributes significantly in the energy range considered. On the contrary, the good overall agreement between theory and experiment suggests that loss-ionization is dominated by independent electron-screened-nuclei interactions (screening mode), rather than by explicit electron-electron interactions (antiscreening mode).

In order to scrutinize this interpretation we have calculated the contribution of antiscreening to the *total* loss-ionization cross section

$$\sigma_{34}^{i} = \sum_{q=1} \sigma_{34}^{q+} \tag{22}$$

in the plane-wave Born approximation (PWBA) [53]. Figure 4 shows a comparison between the results of these calculations and the present experimental and theoretical results obtained by summing up the individual loss-ionization cross sections shown in Fig. 3. Apparently, in accord with our expectations, antiscreening is responsible for a very small fraction of total loss-ionization. If the PWBA cross sections were to be added to the coupled mean-field results, the sum would overestimate the experimental data points at $E_P \geqslant 2$ MeV. However, one should not simply add the cross sections, but instead combine the two calculations at the level of impact-parameter dependent probabilities by appropriate multinomial statistics [23,54], which would result in smaller cross sections. Moreover, it is possible that antiscreening is overestimated in a first-order calculation, since we are concerned with relatively heavy projectile and target species at medium impact energies. Therefore, we conclude that antiscreening might play only a minor role in the present situation.

Returning to Fig. 3 we note that in spite of the good overall agreement between measurements and coupled mean-field calculations for loss-ionization some discrepancies exist. The fact that for $q=4$ and $E_P \geqslant 2.5$ MeV the theoretical results are considerably higher than the experimental ones could signal the limitations of our theoretical description, as overestimations of higher recoil-ion charge states are a well-known deficiency of mean-field models [55]. However, given that no such problems are observed for the pure ionization and the transfer-ionization channels (cf. Figs. 1 and 2) this cannot be stated with certainty.

Contrary to the pure ionization and transfer-ionization channels, calculations lie above experiments in the case of loss-ionization for $q=3$ below $E_P=2$ MeV. One might wonder whether this could compensate for the opposite trends in the other channels if one would sum them up and compare inclusive threefold recoil-ion production. However, the loss cross sections are much smaller than those in the other two sets and do not contribute significantly to the sum. Therefore, a redistribution of threefold recoil-ion production over the three channels would not improve the overall agreement in this case.

Finally, we consider elastic loss, i.e., projectile-electron loss associated with $q=0$. This cross section could not be measured directly, but was obtained by subtracting the sum of all loss-ionization cross sections from the separately measured total electron-loss cross section. The results are shown in Fig. 5. Interestingly, elastic loss decreases as the projectile kinetic energy decreases and is practically equal to zero at $E_P \leqslant 1.5$ MeV.

By contrast, the theoretical cross section curve is rather flat, and the absolute values are similar to those of loss-ionization for $q=1$, which are also included in the figure. This is not surprising given that in an independent electron treatment the corresponding probabilities are basically products of the single-electron-loss probability and the probability to ionize or not to ionize one out of N_T target electrons. In a simple binomial model the target probabilities are given by $p_i^T(1-p_i^T)^{N_T-1}$ and $(1-p_i^T)^{N_T}$, respectively, where p_i^T is the (average) target ionization probability per electron. Obviously, it is impossible that the latter process is zero, while the former is relatively strong. Given that calculations and measurements agree well for $q=1$ one can conclude that the experimental data for elastic loss $q=0$ are not compatible with

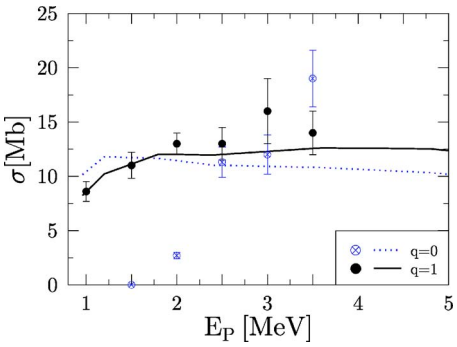

FIG. 5. (Color online) Absolute loss cross sections in C^{3+}-Ne collisions as functions of the projectile kinetic energy for recoil-ion charge states $q=0,1$. The lines represent the theoretical results, and the symbols represent measured values.

the assumption of independent electrons, and are in clear conflict with it below $E_P \approx 2$ MeV. They also show that first-order perturbation theory cannot be valid in this region, since otherwise elastic loss would occur due to the first-order screening process described in the Introduction. Without further information it seems impossible to provide an intuitive physical explanation of the data. At this point we can only state that they might signal the importance of (higher-order) electron correlation effects.

V. CONCLUSIONS

In this paper the C^{3+}-Ne collision system, in which both projectile and target electrons are active, has been investigated. We have measured and calculated charge-state-correlated total cross sections for pure ionization, capture, and loss in the few MeV regime, and have found very good overall agreement between experimental and theoretical results. This provides further evidence for the applicability of the proposed coupled mean-field approach, even if recoil-ion charge states as high as $q=4$ are considered. One can conclude that multiple ionization is strongly dominated by independent interactions for the present case of C^{3+} projectiles.

The only serious qualitative discrepancy between calculations and measurements concerns the elastic electron-loss cross section. While the theoretical curve is rather flat, the experimental cross section decreases to lower energies and is virtually absent at $E_P < 2$ MeV. This behavior cannot be understood in the framework of a mean-field approach, and must therefore be regarded as a manifestation of electron correlation effects, although an intuitive explanation seems impossible without more detailed information.

It is remarkable that the well-known first-order screening and antiscreening processes seem to be of minor importance. This indicates that the realm of perturbation theory is not yet reached at the highest impact energies considered. It would be of interest to extend the energy range of this study in both directions to explore (i) at which higher energies screening and antiscreening modes can be clearly identified, and (ii) down to which energies the present mean-field model gives reliable results.

Finally, we note that double- and even triple-electron loss and capture processes are possible in the present collision system. Unfortunately, charge-state-correlated measurements have not been possible for these channels (see Sec. III). Corresponding data would be very valuable as they would shed further light on the validity and limitations of the present theoretical approach.

ACKNOWLEDGMENTS

This work was supported by the DFG (Germany) and the Brazilian Agencies CNPq, FAPERJ, CAPES, and MCT (PRONEX).

[1] J. S. Yoon and Y. D. Jung, Phys. Plasmas **6**, 3391 (1999).
[2] A. K. Kaminskii and A. A. Vasil'ev, Phys. Part. Nucl. **29**, 201 (1998).
[3] R. D. DuBois *et al.*, Phys. Rev. A **68**, 042701 (2003).
[4] A. C. F. Santos and R. D. DuBois, Phys. Rev. A **69**, 042709 (2004).
[5] R. D. DuBois *et al.*, Phys. Rev. A **70**, 032712 (2004).
[6] D. R. Bates and G. Griffing, Proc. Phys. Soc., London, Sect. A **66**, 961 (1953).
[7] D. R. Bates and G. Griffing, Proc. Phys. Soc., London, Sect. A **67**, 663 (1954).
[8] D. R. Bates and G. Griffing, Proc. Phys. Soc., London, Sect. A **68**, 90 (1955).
[9] E. C. Montenegro, W. E. Meyerhof, and J. H. McGuire, Adv. At., Mol., Opt. Phys. **34**, 249 (1994).
[10] J. H. McGuire, *Electron Correlation Dynamics in Atomic Collisions* (Cambridge University Press, Cambridge, England, 1997), Chap. 8.
[11] H. P. Hülskötter, W. E. Meyerhof, E. Dillard, and N. Guardala, Phys. Rev. Lett. **63**, 1938 (1989).
[12] H. P. Hülskötter *et al.*, Phys. Rev. A **44**, 1712 (1991).
[13] E. C. Montenegro, W. S. Melo, W. E. Meyerhof, and A. G. de Pinho, Phys. Rev. Lett. **69**, 3033 (1992).
[14] R. Dörner *et al.*, Phys. Rev. Lett. **72**, 3166 (1994).
[15] W. Wu *et al.*, Phys. Rev. Lett. **72**, 3170 (1994).
[16] W. Wu *et al.*, Phys. Rev. A **55**, 2771 (1997).
[17] H. Kollmus, R. Moshammer, R. E. Olson, S. Hagmann, M. Schulz, and J. Ullrich, Phys. Rev. Lett. **88**, 103202 (2002).
[18] R. E. Olson, R. L. Watson, V. Horvat, A. N. Perumal, Y. Peng, and T. Stöhlker, J. Phys. B **37**, 4539 (2004).
[19] D. R. Schultz, R. E. Olson, C. O. Reinhold, S. Kelbch, C. Kelbch, H. Schmidt-Böcking, and J. Ullrich, J. Phys. B **23**, 3839 (1990).
[20] J. Fiol, R. E. Olson, A. C. F. Santos, G. M. Sigaud, and E. C. Montenegro, J. Phys. B **34**, L503 (2001).
[21] K. Riesselmann, L. W. Anderson, L. Durand, and C. J. Anderson, Phys. Rev. A **43**, 5934 (1991).
[22] W. S. Melo, M. M. Sant'Anna, A. C. F. Santos, G. M. Sigaud, and E. C. Montenegro, Phys. Rev. A **60**, 1124 (1999).
[23] P. L. Grande, G. Schiwietz, G. M. Sigaud, and E. C. Montene-

gro, Phys. Rev. A **54**, 2983 (1996).
[24] A. B. Voitkiv, G. M. Sigaud, and E. C. Montenegro, Phys. Rev. A **59**, 2794 (1999).
[25] A. B. Voitkiv, N. Grün, and W. Scheid, J. Phys. B **33**, 3431 (2000).
[26] R. D. DuBois, Phys. Rev. A **39**, 4440 (1989).
[27] T. Kirchner and M. Horbatsch, Phys. Rev. A **63**, 062718 (2001).
[28] T. Kirchner, H. J. Lüdde, and M. Horbatsch, Phys. Scr., T **T110**, 364 (2004).
[29] T. Kirchner, M. Horbatsch, and H. J. Lüdde, J. Phys. B **37**, 2379 (2004).
[30] T. Kirchner, Nucl. Instrum. Methods Phys. Res. B **233**, 151 (2005).
[31] J. P. Blaizot and G. Ripka, *Quantum Theory of Finite Systems* (MIT Press, Cambridge, 1986), Chap. 9.
[32] E. K. U. Gross, J. F. Dobson, and M. Petersilka, in *Topics in Current Chemistry*, edited by R. F. Nalewajski (Springer, Heidelberg, 1996), Vol. 181, p. 81.
[33] H. J. Lüdde, in *Many-Particle Quantum Dynamics in Atomic and Molecular Fragmentation*, edited by J. Ullrich and V. P. Shevelko (Springer, Heidelberg, 2003), p. 205.
[34] R. Nagano, K. Yabana, T. Tazawa, and Y. Abe, Phys. Rev. A **62**, 062721 (2000).
[35] X. M. Tong, T. Watanabe, D. Kato, and S. Ohtani, Phys. Rev. A **66**, 032709 (2002).
[36] M. Keim, A. Achenbach, H. J. Lüdde, and T. Kirchner, Phys. Rev. A **67**, 062711 (2003).
[37] M. Keim, A. Achenbach, H. J. Lüdde, and T. Kirchner, Nucl. Instrum. Methods Phys. Res. B **233**, 240 (2005).
[38] T. Kirchner, M. Horbatsch, H. J. Lüdde, and R. M. Dreizler, Phys. Rev. A **62**, 042704 (2000).
[39] E. Engel and S. H. Vosko, Phys. Rev. A **47**, 2800 (1993).
[40] E. Engel and R. M. Dreizler, J. Comput. Chem. **20**, 31 (1999).
[41] H. J. Lüdde, A. Henne, T. Kirchner, and R. M. Dreizler, J. Phys. B **29**, 4423 (1996).
[42] O. J. Kroneisen, H. J. Lüdde, T. Kirchner, and R. M. Dreizler, J. Phys. A **32**, 2141 (1999).
[43] H. J. Lüdde and R. M. Dreizler, J. Phys. B **18**, 107 (1985).
[44] T. Kirchner, Ph.D. thesis, Johann Wolfgang Goethe-Universität, Frankfurt, 1999.
[45] R. L. Becker, A. L. Ford, and J. F. Reading, Phys. Rev. A **29**, 3111 (1984).
[46] A. C. F. Santos, W. S. Melo, M. M. Sant'Anna, G. M. Sigaud, and E. C. Montenegro, Phys. Rev. A **63**, 062717 (2001).
[47] A. C. F. Santos, W. S. Melo, M. M. Sant'Anna, G. M. Sigaud, and E. C. Montenegro, Rev. Sci. Instrum. **73**, 2369 (2002).
[48] H. Luna, E. G. Cavalcanti, J. Nickles, G. M. Sigaud, and E. C. Montenegro, J. Phys. B **36**, 4717 (2003).
[49] M. M. Sant'Anna, H. Luna, A. C. F. Santos, C. McGrath, M. B. Shah, E. G. Cavalcanti, G. M. Sigaud, and E. C. Montenegro, Phys. Rev. A **68**, 042707 (2003).
[50] G. M. Sigaud, M. M. Sant'Anna, H. Luna, A. C. F. Santos, C. McGrath, M. B. Shah, E. G. Cavalcanti, and E. C. Montenegro, Phys. Rev. A **69**, 062718 (2004).
[51] E. G. Cavalcanti, G. M. Sigaud, E. C. Montenegro, M. M. Sant'Anna, and H. Schmidt-Böcking, J. Phys. B **35**, 3937 (2002).
[52] T. Spranger and T. Kirchner, J. Phys. B **37**, 4159 (2004).
[53] E. C. Montenegro and W. E. Meyerhof, Phys. Rev. A **43**, 2289 (1991).
[54] E. C. Montenegro, A. C. F. Santos, W. S. Melo, M. M. Sant'Anna, and G. M. Sigaud, Phys. Rev. Lett. **88**, 013201 (2002).
[55] T. Kirchner, H. J. Lüdde, and M. Horbatsch, Recent Res. Dev. Phys. **5**, 433 (2004).